The 16 valence electronic states of nitric oxide dimer $(NO)_2$

Allan L. L. East
Steacie Institute for Molecular Sciences, National Research Council of Canada, Ottawa, Ontario K1A 0R6, Canada

(Received 3 February 1998; accepted 30 April 1998)

Sixteen electronic states of nitric oxide dimer are investigated using various *ab initio* levels of theory and various orientations of the dimer. These are the states which arise from the mixing of the singly occupied π^*_{NO} orbitals of the monomers, and include all eight states which directly correlate to the $^2\Pi$ ground states of the monomers. Twelve of the sixteen states are significantly multiconfigurational in character, which cause incorrect state orderings at low levels of theory. At several plausible geometries, eight low-lying states are predicted (four singlets and four triplets) within a 1 eV span, hence corresponding to excitations in the *infrared*, while the other eight states (six singlets and two triplets) lie much higher in the far ultraviolet, and in the realm of numerous other electronic states. The results imply, but do not confirm, that the only potential minimum lying below the lowest dissociation asymptote is the cis-ONNO geometrical conformation of the $\tilde{X}\ ^1A_1$ ground state. [S0021-9606(98)30430-4]

I. INTRODUCTION

Nitric oxide dimers $(NO)_2$ are formed when nitric oxide (NO) is cooled, liquified, or frozen. In the gas phase dimer the NO monomers are bound by $710 \pm 40\ cm^{-1}$,[1] which is stronger than usual van der Waals bonds but far weaker than usual covalent ones. Recent experiments on $(NO)_2$ have included gas-phase infrared spectroscopy,[2–4] matrix-infrared spectroscopy,[5–7] gas-phase millimeter-wave spectroscopy[8] and ultraviolet photodissociation,[9,10] and electron[11] and x-ray[12] bombardment of $(NO)_2$ deposited on surfaces.

Despite the experimental interest, the complex electronic nature of this dimer is poorly understood. This is an alarming situation, considering that seven low-lying electronic states lie far below the ultraviolet regime (*vide supra*) and could potentially be involved in the predissociation and matrix-IR investigations.[1,13,14] This paper rectifies this particular and serious dearth of information.

Early theoretical work[15–20] in the dawn of *ab initio* calculations envisaged or examined only the forms of N_2O_2 involving normal N–N single bonds, and several Lewis structures have been (and are still)[21,22] drawn for such forms. These diagrams and many of the early calculated geometries correspond to nonexistent or high energy (2–4 eV) forms of N_2O_2, however,[23,24] and when experimental evidence for the only known form of N_2O_2 established an N–N distance of over 2 Å,[25–27] these early theoretical studies proved to be no help in understanding this low-energy, weakly-bound isomer. The experimental geometry[2] has now been correctly reproduced by theory,[28,29] with the bonding being due to coupling of the unpaired π^*_{NO} electrons of the monomers, leaving essentially triple bonds for each monomer. There is considerable speculation of alternative geometrical arrangements of the dimer, due to density functional calculations[7,30,31] and old[32] and current[5–7] observations of multiple matrix-IR peaks, but these have yet to be established for the gas-phase dimer, either by experiment or improved *ab initio* work.

Most current theoretical computations have been concerned solely with the $\tilde{X}\ ^1A_1$ ground state. Many of these studies have used levels of theory (such as density functional theory) which predict a *triplet* ground state, contrary to experimental evidence. Beyond the $\tilde{X}\ ^1A_1$ state, Dykstra and co-workers[18] and Salahub and co-workers[30] have each investigated a low-lying triplet state, and Bardo[19] investigated an alternative singlet state, at low levels of theory. Models for some of the expected electronic states (correlating them to states of the dissociated products) have been advanced.[1,26] Notwithstanding the study of high-energy core-excitation states by Handy and co-workers,[12] only the 1981 study of Ha[33] and the 1975 calculations of Mason[34] exist as resources for the energies of more than two of the low-lying states of $(NO)_2$. Although these works did predict electronic states as low as in the near infrared, the results of the current study demonstrate that many of these early predictions were quite inaccurate.

The goal of this paper is to clarify the complex electronic problem of $(NO)_2$ and provide reasonably accurate (± 0.2 eV) state energies for the first time. Sixteen electronic states are investigated, and at three different monomer alignment possibilities in order to address the aforementioned speculation of alternative geometrical arrangements. Various levels of theory are employed in order to demonstrate their powers and weaknesses when applied to this very demanding system.

II. MOLECULAR ORBITAL MODEL

The electronic states of $(NO)_2$ are best understood by relating them to the states of the dissociated NO monomers. Spin–orbit coupling effects are neglected (the accuracy in this work will be too coarse for this) but briefly addressed in the Appendix. In Fig. 1 the molecular orbital configurations

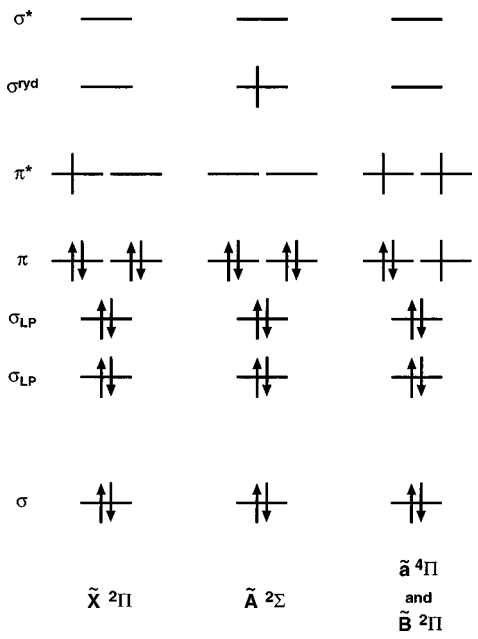

FIG. 1. Molecular orbital electron configurations for four states of NO monomer. Note that three other states ($^2\Pi, ^2\Pi, ^2\Phi$) also arise from a $\pi^3\pi^{*2}$ occupation. The four 1*s* core electrons are not shown.

of the four lowest electronic states of NO monomer are shown. According to molecular orbital theory, the valence orbitals of the monomer consist of a σ_{NO} bonding orbital, two σ lone pair (nonbonding) orbitals, two π_{NO} bonding orbitals, two π^*_{NO} antibonding orbitals, and a σ^*_{NO} antibonding orbital. In the $\tilde{X}\ ^2\Pi$ ground state of NO there is one odd electron in the pair of doubly degenerate π^*_{NO} orbitals. The $A\ ^2\Sigma$ state is a Rydberg state arising from promotion of this π^*_{NO} electron to an *s*-type Rydberg orbital, while the $\tilde{a}\ ^4\Pi$ and $\tilde{B}\ ^2\Pi$ non-Rydberg states arise from $\pi_{NO} \rightarrow \pi^*_{NO}$ excitation.[35,36] These three monomer excited states have adiabatic excitation energies (T_0 values) between 4.7–5.7 eV (38 000–46 000 cm^{-1}),[36,37] and hence this 4.7–5.7 eV range represents a zeroth-order approximation of the energies of corresponding dimer states. Also possible are dimer states which would correspond to ionic $NO^+ + NO^-$ dissociation asymptotes which lie at 11.0 eV ($^3\Sigma^-$ NO^-), 11.7 eV ($^1\Delta$ NO^-), and 12.1 eV ($^1\Sigma^+$ NO^-).[38,39]

Omitted from this broad description, however, is the fact that *more than one state* will arise from each combination of NO monomers described above, including the association of two ground-state monomers ($\tilde{X}+\tilde{X}$). According to molecular orbital theory, $\tilde{X}+\tilde{X}$ should produce dimer states which qualitatively consist of 28 ''core'' electrons, which behave as slightly perturbed electrons of NO^+ ions, and two ''valence'' electrons, which are able to access the four orbitals arising from mixing of the π^*_{NO} monomer orbitals. In our zeroth-order picture of noninteracting monomers, these states are *degenerate*, and this is the fundamental underlying reason for the existence of electronic states at energies far below the ultraviolet. At first count, the possibilities for two electrons in 4 orbitals (8 spin–orbitals) are $\binom{8}{2} = 28$ valid determinant wave functions, and 16 electronic states (10 singlets and 6 triplets). However, as will be demonstrated in Sec. IV,

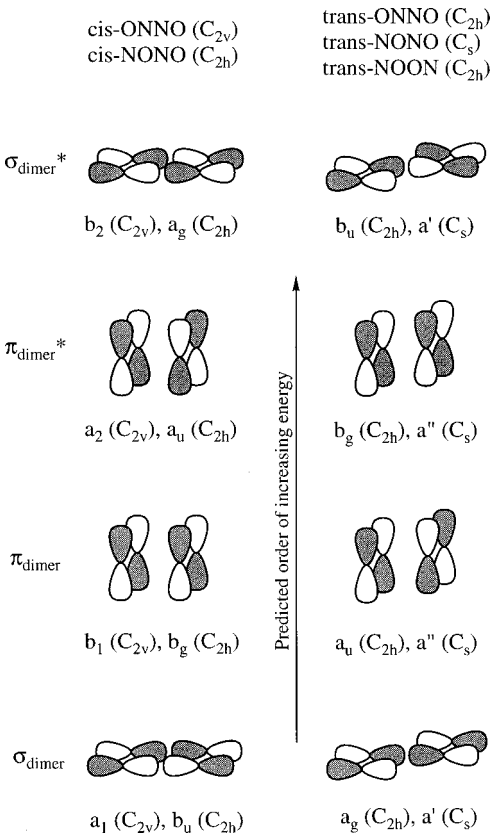

FIG. 2. The four molecular orbitals accessed by the two labile electrons in the 16 valence electronic states of $(NO)_2$. These diagrams are idealized; for instance the effects due to electronegativity differences of N vs O are not shown.

only 8 of these 16 states can directly correlate to $\tilde{X}\ ^2\Pi + \tilde{X}\ ^2\Pi$, with the other 8 corresponding to ionic $NO^+ + NO^-$ asymptotes.

For the other monomer combinations, $\tilde{X}+\tilde{A}$ directly (adiabatically) gives rise to 8 Rydberg dimer states (4 singlets and 4 triplets), while $\tilde{X}+\tilde{a}$ and $\tilde{X}+\tilde{B}$ directly correlate to 32 non-Rydberg states (8 quintuplets, 16 triplets, and 8 singlets). This congestion of states in the mid- to far-ultraviolet causes considerable difficulties in attempts to calculate their spectral locations or other properties, and hence this paper restricts itself to the 16 valence states which are candidates for the much lower lying $\tilde{X}+\tilde{X}$ states.

For the dimer, the term valence will be used to describe the two outer electrons, the four orbitals they may occupy, and hence, the resulting 16 states. (The two σ^*_{NO} monomer orbitals are also valence orbitals for the dimer, and are included in the multireference calculations, but contribute very little to these sixteen states.) Sketches of these four orbitals appear in Fig. 2. Note that the orbital (and state) symmetries depend upon the geometrical arrangement. One would expect the in-plane orbitals to mix (overlap) more than the out-of-plane ones, and hence, one can order these four orbitals in energetic preference immediately and estimate an order for the resulting states. For instance, for cis-ONNO, the ground state is predicted to involve double occupation of the $a_1\sigma_{dimer}$-type orbital, followed by a singlet–triplet pair of states involving single occupation of the a_1 and b_1 orbitals.

This model proved extremely helpful for locating the various states.

III. THEORETICAL METHODS

All calculations were performed with MOLPRO94.[40] The methods employed were: Single- or two-configuration Hartree–Fock self-consistent field (HF-SCF), complete active space SCF (CASSCF),[41,42] Kohn–Sham density functional theory (DFT),[43] single-configuration coupled cluster [CCSD(T)],[44,45] and internally contracted multireference configuration interaction (MRCISD).[46,47] The principal calculations were CASSCF and MRCISD vertical excitation energies, although some properties were also determined using MRCISD.

The single-configuration HF-SCF calculations involved single Slater determinants except for open-shell singlet states, which require an equal mixture of two Slater determinants and could be so obtained with the MULTI algorithm of MOLPRO. Spatial orbitals for electrons of either spin were restricted to be identical (RHF). The CASSCF calculations used as the active space 2 electrons in the six dimer valence orbitals (from the π^*_{NO} and σ^*_{NO} monomer orbitals). The DFT calculations employed the 1988 Becke gradient-corrected exchange[48] and the 1988 Lee–Yang–Parr gradient-corrected correlation[49,50] energies (BLYP). The CCSD(T) and MRCISD calculations involved all single and double excitations from the reference configuration(s). For CCSD(T) the traditional correction for triple excitations was included,[51] orbitals were taken from the RHF-SCF calculation, and for open-shell configurations the algorithm forces only the linear part of the wave function to be a proper spin eigenfunction.[52] For MRCISD the reference configurations for a particular state consisted of all configurations present in the CASSCF calculations, and the orbitals were taken from the CASSCF calculation for that state.

The primary basis set employed was the cc-pVTZ basis set of Dunning and co-workers.[53] Also tested were the cc-pVDZ, aug-cc-pVDZ, and aug-cc-pVTZ sets,[54] which gave very similar results for the electronic state spacings and orderings. However, diffuse functions (such as in the aug-sets), which have Rydberg-orbital character, caused many convergence problems for the upper 8 states (which are predicted to lie near Rydberg states), and hence were not employed in general.

Figure 3 displays the four dimer arrangements we considered to be most likely candidates for $\tilde{X}+\tilde{X}$ minima: Two side-on forms (cis-ONNO, cis-NONO), and two staggered forms (trans-ONNO, trans-NONO). These four were chosen because of the logical anticipation of bonding involving the π^*_{NO} monomer orbitals. Bond lengths and angles were taken from the best experimental result for cis-ONNO,[2] because the *ab initio* geometry predictions possessed nontrivial variations caused by the small binding energy (see Sec. IV C). Energies for all 16 states of interest were determined at three of these forms. Unfortunately, the trans-NONO form has less symmetry, greatly limiting successful wave function convergence and leaving us little indication that we were finding the lowest states for this form, and hence, no trans-NONO results can be presented at this time.

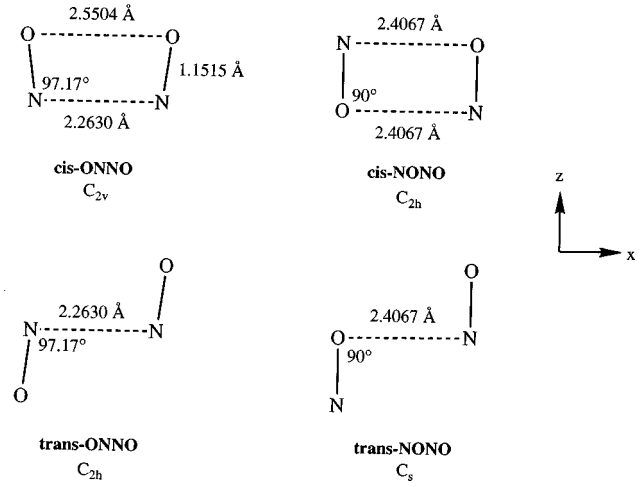

FIG. 3. The four geometries chosen for the vertical excitation computations. The cis-ONNO structure is from Ref. 2; the other structures are derivatives of this.

The higher 8 states are predicted to lie not only near Rydberg states, but also near states which arise from $\pi_{NO}\rightarrow\pi^*_{NO}$ monomer excitation. A larger CASSCF active space which incorporates such excitations (10 electrons in 10 orbitals) was briefly tested. It was found to be unnecessary for the lowest 8 states (no new configuration coefficient larger than 0.07 for the particular triplet state we tested), but indeed there was a noticeable change in wave function character for the test member of the upper 8 states, indicating that the smaller CASSCF active space is less appropriate for these higher 8 states, and that their energy predictions are somewhat less accurate than those of the lower 8 states. It is anticipated, however, that the effect upon relative electronic energies of increasing the CASSCF active space from 2 to 10 electrons cannot be so large as to bring some of these states down to those of the lower 8 (which would require a 6 eV lowering).

Several root-flipping problems were encountered during CASSCF runs. In most cases, it was appropriate to fully weight the anticipated root; for instance, requesting full weight of the third lowest root of $^1A_1$ symmetry for cis-ONNO was correct for the third lowest $^1A_1$ state in our 16-state subset. However, due to the effects of orbital rotation, there were three cases (for cis-ONNO these would be the lowest two states of $^1A_1$, $^1B_2$, and $^3B_2$ symmetry, respectively) at each geometry in which both states had to be obtained with the *lowest-root* algorithm. The evidence for root-flipping came from performing state-averaged CASSCF runs with differing weight ratios.[55]

Transition dipole moments were computed via MRCISD based on 50:50 state-averaged CASSCF calculations, due to the need for common orbitals. To determine the MRCISD coefficients for each state prior to computing the expectation value, the contracted pairs were generated from only one of the two reference states, i.e., upper for upper and lower for lower.

TABLE I. Valence states of NO dimer, cis-ONNO configuration.[a,b]

State label	State type	E(eV) HF-SCF	E(eV) CASSCF	CI vector[c]
1	$^1A_1$	2.57	0.00	0.88(2000)−0.47(0200)
2	$^1B_1$	3.39	0.50	0.83(1010)−0.55(0101)
3	$^3B_1$	2.78	0.38	0.85(1010)−0.53(0101)
4	$^1A_1$	4.60	0.57[d]	largely (0020)
5	$^1A_2$	4.23	0.70	0.79(1001)−0.62(0110)
6	$^3A_2$	3.67	0.69	0.79(1001)−0.61(0110)
7	$^1B_2$	8.44	8.36	1.00(1100)
8	$^3B_2$	0.84	0.83	1.00(1100)
9	$^1B_2$	9.13	9.07	1.00(0011)
10	$^3B_2$	0.61	0.61	1.00(0011)
11	$^1A_2$	6.36	9.33	0.79(0110)−0.61(1001)
12	$^3A_2$	5.76	8.28	0.80(0110)−0.60(1001)
13	$^1A_1$	6.44	9.58	0.67(0002)+0.57(0020)-0.41(0200)-0.21(2000)
14	$^1B_1$	7.30	9.65	0.83(0101)−0.55(1010)
15	$^3B_1$	6.63	8.61	0.84(0101)−0.53(1010)
16	$^1A_1$	8.70	10.74	0.67(0200)+0.47(0002)+0.41(0020)+0.38(2000)

[a]Results were obtained using the cis-ONNO geometry shown in Fig. 3.
[b]The zero of energy is −258.573 399 a.u. (the lowest cis-ONNO CASSCF energy).
[c]The configuration label ($abcd$) indicates which of the four available orbitals are occupied by the two labile electrons: ($a_1b_2b_1a_2$). The leading one is the one used in the HF-SCF calculations.
[d]This CASSCF energy was obtained by quadratic extrapolation of energies from four state-averaged CASSCF runs, in which the energy of the ground state was simultaneously optimized with weights of 50, 30, 20, and 10 percent.

IV. RESULTS AND DISCUSSION

A. CASSCF vertical excitation energies

All 16 electronic states were located with HF-SCF and CASSCF calculations at three of the four fixed geometries (Fig. 3). The results for the state energies at the three chosen geometries are tabulated in Tables I–III and plotted in Fig. 4. A close-up of the CASSCF results for the lower 8 states appears in Fig. 5. The zero of energy is taken to be the energy of the $\tilde{X}\ ^1A_1$ state of cis-ONNO. Attention is drawn to several interesting aspects.

(1) The HF approximation (which lacks both dynamical and nondynamical Coulombic electron correlation) is severely lacking in quality for 12 of these 16 states. The CASSCF calculations incorporate the nondynamical correlation, and this is clearly important in these 12 cases, as shown by the splitting of the energies of states of common symmetry by several eV, and by the dominant mixing coefficients in the configuration interaction (CI) eigenvectors in the Tables.

(2) The 16 states, when computed with nondynamical correlation, coalesce into two sets of 8 states. The lower 8

TABLE II. Valence states of NO dimer, cis-NONO configuration.[a,b]

State label	State type	E(eV) HF-SCF	E(eV) CASSCF	CI vector[c]
1	^1A_g	3.25	0.19	0.84(0020)−0.54(2000)
2	^1A_u	3.89	0.49	0.81(0011)−0.59(1100)
3	^3A_u	3.26	0.42	0.81(0011)−0.58(1100)
4	^1A_g	4.96	0.49	0.74(0002)−0.67(0200)
5	^1B_g	4.39	0.57	0.76(0110)−0.64(1001)
6	^3B_g	3.82	0.58	0.78(0110)+0.63(1001)
7	^1B_u	8.73	8.60	0.99(1010)
8	^3B_u	0.59	0.58	1.00(1010)
9	^1B_u	9.39	9.31	1.00(0101)
10	^3B_u	0.51	0.51	1.00(0101)
11	^1B_g	6.10	9.34	0.76(1001)+0.64(0110)
12	^3B_g	5.51	8.31	0.78(1001)−0.63(0110)
13	^1A_g	6.08	9.48	0.64(2000)−0.47(0200)−0.42(0002)+0.41(0020)
14	^1A_u	6.68	9.51	0.81(1100)+0.59(0011)
15	^3A_u	6.06	8.48	0.81(1100)+0.58(0011)
16	^1A_g	7.72	10.50	0.53(0200)+0.56(2000)+0.48(0002)+0.38(0020)

[a]Results were obtained using the cis-NONO geometry shown in Fig. 3.
[b]The zero of energy is −258.573 399 a.u. (the lowest cis-ONNO CASSCF energy).
[c]The configuration label ($abcd$) indicates which of the four available orbitals are occupied by the two labile electrons: ($a_ga_ub_ub_g$). The leading one is the one used in the HF-SCF calculations.

TABLE III. Valence states of NO dimer, trans-ONNO configuration.[a,b]

State label	State type	E(eV) HF-SCF	E(eV) CASSCF	CI vector[c]
1	^1A_g	3.25	0.21	0.85(2000)−0.53(0020)
2	^1A_u	3.86	0.53	0.79(1100)−0.61(0011)
3	^3A_u	3.25	0.44	0.81(1100)−0.59(0011)
4	^1A_g	4.78	0.41	0.75(0200)−0.66(0002)
5	^1B_g	4.32	0.55	0.76(1001)−0.65(0110)
6	^3B_g	3.78	0.57	0.77(1001)+0.64(0110)
7	^1B_u	7.75	7.67	1.00(1010)
8	^3B_u	0.61	0.60	1.00(1010)
9	^1B_u	8.88	8.81	1.00(0101)
10	^3B_u	0.43	0.43	1.00(0101)
11	^1B_g	5.78	8.87	0.76(0110)+0.64(1001)
12	^3B_g	5.19	7.87	0.77(0110)−0.63(1001)
13	^1A_g	5.93	10.09	0.57(0002)+0.53(0200)+0.50(0020)+0.34(2000)
14	^1A_u	6.39	9.11	0.79(0011)+0.59(1100)
15	^3A_u	5.73	8.08	0.81(0011)+0.59(1100)
16	^1A_g	7.38	8.96	0.79(0020)+0.51(2000)−0.21(0002)−0.19(0200)

[a]Results were obtained using the trans-ONNO geometry shown in Fig. 3.
[b]The zero of energy is −258.573 399 a.u. (the lowest cis-ONNO CASSCF energy).
[c]The configuration label ($abcd$) indicates which of the four available orbitals are occupied by the two labile electrons: ($a_g a_u b_u b_g$). The leading one is the one used in the HF-SCF calculations.

are grouped to within 1 eV, while the higher 8 are grouped to within 3 eV, and the two groups are completely separated by 7 eV at each geometry tested.

(3) The 8 high-lying states lie roughly between 7 and 10 eV, which should place them amongst several other electronic states which correspond to excited states of one of the monomers.

(4) Examples of both strong and minor coupling between zeroth-order states of common spin and spatial symmetry are seen, and can be understood from orbital overlap arguments. For example, the four $^1A_1$ configurations of cis-ONNO can be separated into two pairs due to an extra internal symmetry in the wave function. Two of the configurations have an in-plane (σ_{dimer}-type) orbital (either a_1 or b_2) as its highest-occupied molecular orbital (HOMO). When doubly occupied, these orbitals have a considerable degree of overlap, and the net coupling between these two configurations is strong. The same argument applies for the other two configurations, which have for HOMO's the out-of-plane (π_{dimer}-type) b_1 and a_2 orbitals, respectively. However, an out-of-plane orbital has very little overlap with an in-plane orbital, and hence these latter two configurations interact very little with the previous two.

(5) The 4 states numbered 7–10 in the tables (the B_2 states for cis-ONNO) are peculiar. They are unaffected by nondynamical correlation, due to very little configuration

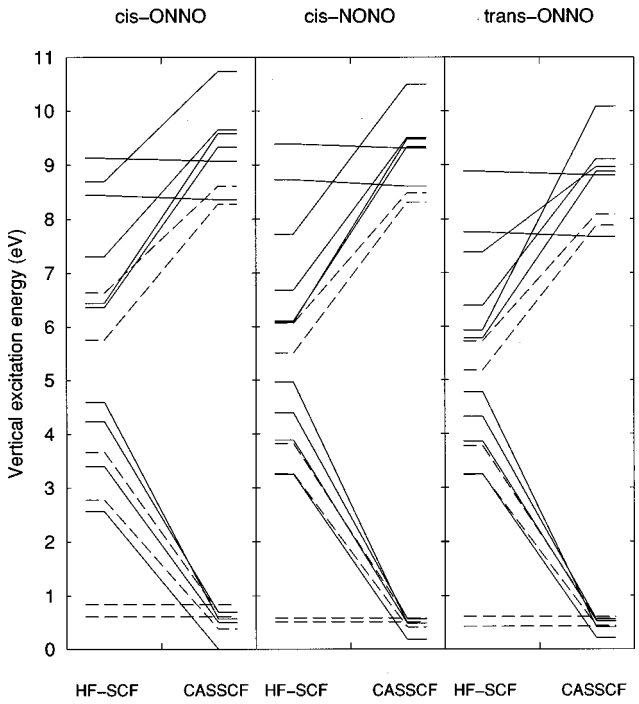

FIG. 4. Computed electronic state energies of all 16 states, before and after CASSCF interaction of the simple HF wave functions. The six triplet states are shown with the dashed lines. Energies are to scale, and relative to the lowest CASSCF energy obtained (the $\tilde{X}\ ^1A_1$ state of cis-ONNO).

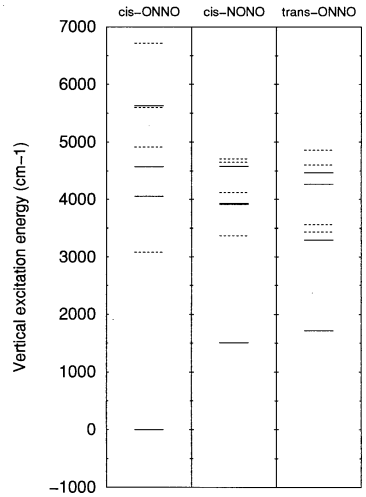

FIG. 5. Close-up of the CASSCF energies of the eight lowest states in Fig. 4. Triplet states are again shown with dashed lines.

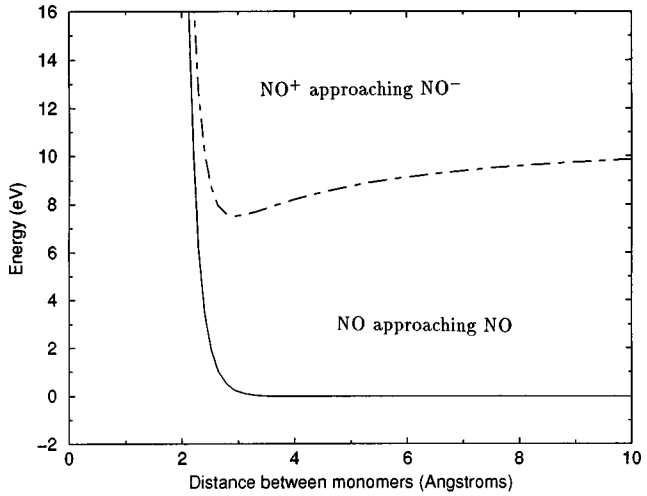

FIG. 6. The ''physicist's model'' describing the underlying dissociation potentials for the upper 8 states, $4\epsilon(\sigma/r)^{12}-1/r$, and lower 8 states, $4\epsilon(\sigma/r)^{12}-4\epsilon(\sigma/r)^{6}$.

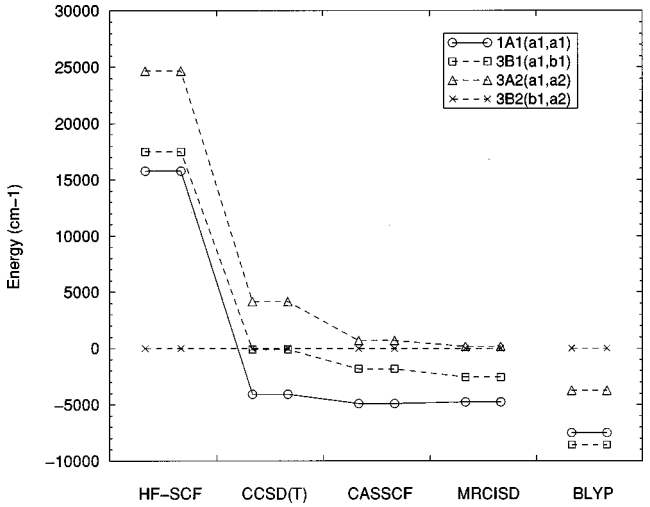

FIG. 7. Energies of four states of cis-ONNO using different levels of theory. All employed the cc-pVTZ basis set. For each state, the dominant orbital occupation of the two labile electrons is indicated in the legend box.

overlap, similar to certain pairs of $^1A_1$ states mentioned in the preceding point. Rather more striking, however, is that (a) at the HF level they already lie in the regions of coalescence, and (b) instead of a low-lying ($^3B_2$, $^1B_2$) pair and a similar high-lying pair, the two $^3B_2$ states are low and the two corresponding $^1B_2$ states are much higher!

Ionic dissociation asymptotes are reponsible for most of these interesting observations. Since a $^2\Pi$ monomer has fourfold degeneracy, two such monomers give rise to only 16 electronic configurations. The other 12 which are involved in the description of the dimer states in this work come from the ionic asymptotes: 6 from $^3\Sigma^-\mathrm{NO}^-+\mathrm{NO}^+$ (either monomer *A* or monomer *B* can be the anion), 4 from $^1\Delta\mathrm{NO}^-+\mathrm{NO}^+$, and two from $^1\Sigma^+\mathrm{NO}^-+\mathrm{NO}^+$. In a ''supermolecule'' consideration of these 12 wave functions, these result in two triplet states and six singlet states, *matching exactly the state composition of the group of 8 higher dimer states*. A supermolecule consideration of the symmetrized combinations of the 16 determinants from $^2\Pi$ NO+$^2\Pi$ NO produces four triplet and four singlet states, matching the composition of the group of 8 lower states of the dimer.

Although the ionic asymptotes are predicted to be 11 to 12 eV above the $\tilde{X}+\tilde{X}$ neutral one, the long-range $1/r$ potential of the ions accounts perfectly for the 7–10 eV energy range for these 8 states. In Fig. 6 a ''physicist's model'' of these dissociation potentials is presented. The lower curve is a Lennard-Jones 6-12 potential

$$E=4\epsilon[(\sigma/r)^{12}-(\sigma/r)^{6}], \tag{1}$$

with parameters for CO (ϵ=0.000 33 a.u., σ=3.62 Å).[56] The upper curve takes the same repulsive $4\epsilon(\sigma/r)^{12}$ term but adds $-1/r$ for the electrostatic attraction between a positive and negative ion of unit charge. The only variable is the spacing of the asymptote energies, taken to be 11 eV.[39] There are no covalent or ''chemical'' forces in these curves, and the small Lennard-Jones minimum is not visible on this scale. It should be clear to the reader that the energies of these 16 valence dimer states, estimated well by CASSCF, are dominated firstly by the dissociation asymptotes, and only secondly by inter- and intra-asymptote coupling.

States 7–10 lie in their correct regions even at HF-SCF level because molecular orbital theory accounts (some would say overaccounts) for contributions from ionic asymptotes.[57] The other 12 states do not behave correctly at HF-SCF because one-configuration wave functions cannot describe these states correctly. When employing molecular orbital theory for these states, most zeroth-order wave functions correspond to *both* physical asymptotes, and hence, must be coupled to describe states relating to either regime.

B. MRCISD and other methods

We moved on to contrast the CASSCF energies with energies at BLYP-DFT, CCSD(T), and MRCISD levels of theory, using the cis-ONNO geometry only. Only four states could be accessed with the available CCSD(T) code, and the results for these four appear in Fig. 7. The DFT results are placed separately because its energies are density based rather than orbital based. The energies are plotted relative to the $^3B_2$ state energy, rather than the $\tilde{X}$ $^1A_1$ energy, because this state is least affected by improvements in theoretical method.

The MRCISD results should be the most accurate, and hence, the CASSCF results are strongly supported, in state orderings and in relative spacings. To calibrate the accuracy of the CASSCF and MRCISD predictions, the adiabatic excitation energies of NO monomer from the $\tilde{X}$ state to the $\tilde{a}$ and $\tilde{B}$ states (see Fig. 1) were computed with CASSCF (5 electrons in 5 orbitals active) and MRCISD (using reference configurations from the CASSCF active space), with results within 1700 cm^{-1} (0.2 eV) of experiment[36,37] for CASSCF, and within 800 cm^{-1} (0.1 eV) for MRCISD. One might, therefore, estimate similar 0.2 and 0.1 eV accuracies for the CASSCF and MRCISD predictions of the dimer electronic state energies.

The single-reference CCSD(T) and DFT methods demonstrate remarkable abilities to incorporate multireference

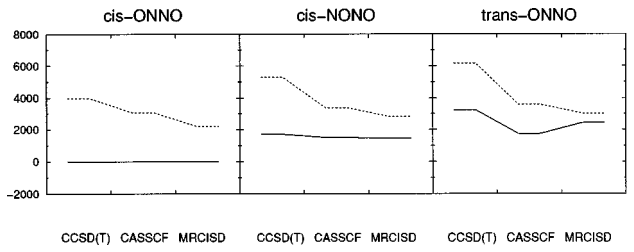

FIG. 8. Energies of the states labeled 1 and 3 in Tables I–III, relative to the ground-state cis-ONNO energy, at various geometries and levels of theory. State 3, a triplet state, is again shown with a dashed line.

character, which brings the energies of the $^1A_1$, $^3A_2$, and $^3B_1$ states down to that of the $^3B_2$ state in the figure. Density functional theory, however, scrambles the state ordering, and even predicts a triplet ground state that is different than the triplet favored by basic HF calculations. This result is not particular to BLYP,[30] and therefore, it is DFT that is inherently failing for relative electronic energies for this system.

Next we addressed the relative energies of the various geometric conformations. Energies of states 1 and 3 (as labeled in Tables I–III) were calculated at the cis-NONO and trans-ONNO geometries as well, using CASSCF, CCSD(T), and MRCISD. The results for all three geometries are plotted in Fig. 8. Improvements from CASSCF to MRCISD tend to be 1000 cm^{-1} or less, reducing the singlet–triplet gap, but not the ground-state energy of the two alternative geometries relative to cis-ONNO.

Hence, barring unforseen effects due to alterations in geometry from those of Fig. 3, two conclusions are made. First, the CASSCF energies of the low 8 states in Tables I–III and Fig. 5 have roughly 0.2 eV (1600 cm^{-1}) accuracy. This demonstrates that the outmoded CISD results of Ha[33] have errors varying from 0.3 to 4.2 eV. Secondly, recalling that the $\tilde{X}+\tilde{X}$ dissociation asymptote is thought to lie less than 800 cm^{-1} above the ground state of cis-ONNO, the the current results suggest that *all* trans-ONNO and cis-NONO states, and all cis-ONNO states except the ground state, are thermally unstable (likely repulsive) with respect to dissociation to two ground-state monomers. It seems likely that all of these states are thermally unstable at other geometries (such as trans-NONO) as well.

To present final predictions for the lowest 8 electronic states of $(NO)_2$, we have computed MRCISD vertical excitation energies, dipole moments, and transition dipole moments for the cis-ONNO conformation, with the results appearing in Table IV. The dipole moments should be considered as ''instantaneous'' ones, since the seven excited states are thermally unstable and possibly purely dissociative. Instantaneous dipole moments were obtained for all 16 states at the CASSCF level of theory, and while these absolute values appear poor (consistently 0.4 Debye more negative than the MRCISD values for the low 8 states), the CASSCF results predict all of the higher 8 states to have dipole moments roughly 0.6 Debye more positive than all of the lower 8 states. The transition dipole moments convert to oscillator strengths (*f*-values) of $2\times10^{-6}(^1B_1)$ and $2\times10^{-8}(2\,^1A_1)$. Note that Mason[34] did report rising absorption above 1160 nm (below 8600 cm^{-1}) with an *f*-value above 10^{-6} in the liquid.

TABLE IV. Final results (cc-pVTZ MRCISD) for the low 8 electronic states of $(NO)_2$.[a]

State label	State type	$E(cm^{-1})$	μ(Debye)[b]	TDM(Debye)[c]
8	$^3B_2$	7050	−0.280	···
5	$^1A_2$	4990	−0.207	···
6	$^3A_2$	4920	−0.214	···
10	$^3B_2$	4760	−0.193	···
4	$^1A_1$	4130[d]	−0.17[d]	(0,0,−0.0035)
2	$^1B_1$	3140	−0.180	(0,+0.0330,0)
3	$^3B_1$	2200	−0.181	···
1	$^1A_1$	0	−0.238	···

[a]Results were obtained using the cis-ONNO geometry shown in Fig. 3.
[b]Dipole moment, for this particular geometry.
[c]Transition dipole moment from the ground state. Five of the transitions are forbidden in the usual approximation.
[d]These values were obtained by quadratic extrapolation using orbitals from four state-averaged CASSCF runs in which the energy of the ground state was simultaneously optimized with weights of 50, 30, 20, and 10 percent.

Finally we offer a comment on the predissociation of $(NO)_2$ in the infrared spectrum. Our best result for the vertical excitation energy from the ground state of cis-ONNO to the lowest excited state (a $^3B_1$ state) is 2200 cm^{-1}, with possibly ±1000 cm^{-1} uncertainty. The next lowest state is most likely a $^1B_1$ state, another 1000 cm^{-1} or so higher in energy. Hence, it would appear that these two (and likely only the $^3B_1$ state) are possible candidates for nonadiabatic transitions from a ν_1- or ν_5-excited ground electronic state, since these fundamentals lie at 1868 and 1789 cm^{-1}, respectively.[4]

C. Geometry variations

While geometry optimization was not considered important to this study, new determinations of the ground-state cis-ONNO geometry were obtained, and it would seem prudent to make some pertinent comments.

Table V is an updated table of the best predictions of the ground-state cis-ONNO geometry. The CCSD(T) and MRCISD+Q methods were capable of obtaining the geometry accurately [r(N–N) within 6%]. DFT consistently predicts r(N–N) to be over 10% too small,[7,30,58] our particular MRCISD optimization gave an r(N–N) value which is 10% too large, and our aug-cc-pVDZ CASSCF optimization simply dissociated, implying that CASSCF may not produce a bound dimer. This is a clear indication that quantum chemistry energy methods have their strengths and weaknesses! This molecule accentuates these problems, and for its investigation it should be considered quite acceptable to use different levels of theory for the properties for which they are best suited. The possible failure of CASSCF to predict a 0.1 eV bound minimum does not mean it is incapable of 0.2 eV accuracy in electronic excitation energies, nor should the difficulties of single-reference CCSD(T) or DFT in $(NO)_2$ excited state estimation cause one to completely dismiss their potential ability to describe weakly bound ground-state minima, because these quantities in $(NO)_2$ have very little in

TABLE V. Best predicted geometries for $(NO)_2$.[a]

Method[b]	Basis set	Source	r_{NN}	r_{OO}	r_{NO}	θ_{NNO}
2RCISD	DZP	Ha (Ref. 33)	2.39	2.39	1.19	90.0
8RCISD	aug-cc-pVDZ	this work	2.492	2.651	1.142	94.0
CCSD(T)	DZP	Lee-Rendell-Taylor (Ref. 28)	2.354	2.572	1.180	95.3
CCSD(T)	aug-cc-pVDZ	this work	2.227	2.480	1.169	96.2
CCSD(T)	cc-pVTZ	this work	2.164	2.454	1.157	97.2
2RCISD+Q	$4s3p2d$	Roos and co-workers (Ref. 29)	2.253	2.545	1.149	97.3
2R-ACPF	$6s5p3d2f$	Roos and co-workers (Ref. 29)	2.284	2.528	1.149	96.1
expt.		McKellar–Watson–Howard (Ref. 2)	2.2630	2.5504	1.1515	97.17

[a]Bond lengths in Å, angles in degrees.
[b]For the multireference methods, the number of reference configurations is indicated.

common; one requires accurate estimate of nondynamical correlation while the other puts a larger demand on dynamical correlation. There exist more computationally difficult or expensive methods (MRCISD, CASMP2, full CI) which may describe all energetic aspects of $(NO)_2$ to some satisfying uniform threshhold of accuracy, but one should be aware that this could be considered a waste of shared computer resources since they are not always needed to address important subsets of the chemistry or physics of a molecule.

The last question we wish to address here is the variation of excitation energies with small changes in geometry, since our choices of geometry in this study were quite arbitrary. Hence we computed additional cc-pVTZ CASSCF excitation energies of state 1 to state 3 at all three geometric forms, but now using bond lengths and angles from the optimized aug-cc-pVDZ MRCISD cis-ONNO geometry. The 0.23 Å r(N–N) increase is the largest geometric change from the structures used earlier, and the effects were the reduction of relative CASSCF conformer energies by 300–700 cm^{-1} and reduction of the state 1-state 3 excitation energies by 400–1000 cm^{-1}. These reductions are guided by the dissociation asymptote, since for very large r(N–N) values all these energies converge. This should give the reader a rough indication of the dependence of the electronic state energies upon intermonomer distance, if desired.

V. SUMMARY

Sixteen electronic states of nitric oxide dimer were investigated using various *ab initio* levels of theory and three fixed orientations of the dimer. These are the states which arise in molecular-orbital theory from mixing of the singly occupied π^*_{NO} orbitals of the monomers. The states group into two collections, because 8 of these states (4 singlets and 4 triplets) correlate to dissociated $^2\Pi$ monomer states, while the other 8 states (6 singlets and 2 triplets) correlate to $NO^+ + NO^-$ states. The low 8 states are predicted to lie within 1 eV of the ground state at all three chosen geometries, while the high 8 states lie significantly higher in the realm of numerous other electronic states.

Twelve of the sixteen states are significantly multiconfigurational in character, which cause incorrect state orderings at low levels of theory. For the low 8 states, the CASSCF and MRCISD results were found to be the most reliable of the five methods we tested. The low-8 state ordering could not be definitively determined due to the narrow energy span, although for cis-ONNO the ordering of the lowest four ($\tilde{X}\ ^1A_1, ^3B_1, ^1B_1, ^1A_1$) should be correct.

The results suggest that only the ground state should have a minimum below the lowest dissociation asymptote, and only in the cis-ONNO conformation. The lowest $^3B_1$ and $^1B_1$ states are sufficiently low (2200 and 3140 cm^{-1}, respectively, from Table IV) to be candidates for nonadiabatic transitions from the ν_5- or ν_1-excited ground state.

ACKNOWLEDGMENTS

A. R. W. McKellar, K. P. Huber, J. K. G. Watson, A. Stolow, H.-P. Loock, and P. R. Bunker are thanked for valuable discussions.

APPENDIX: SPIN–ORBIT COUPLING EFFECTS

Spin–orbit effects were neglected in the computations in this work. The observed effect upon the $\tilde{X}\ ^2\Pi$ monomer state is to create $^2\Pi_{1/2}$ and $^2\Pi_{3/2}$ states split by 120 cm^{-1}. This splits the $^2\Pi$ NO+$^2\Pi$ NO dissociation asymptote into three. The lowest, $^2\Pi_{1/2}+{}^2\Pi_{1/2}$, consists of 4 electronic configurations and two states (a supermolecule singlet and a supermolecule triplet). The highest asymptote, $^2\Pi_{3/2}+{}^2\Pi_{3/2}$, is similarly composed. The middle $^2\Pi_{1/2}+{}^2\Pi_{3/2}$ asymptote produces two singlets and two triplet states (8 electronic configurations).

In most of our figures, and certainly to our current level of computational accuracy, this splitting is too small to be noticeable. The splitting represents 20% of the binding energy of the dimer ground state, however, and can create rather interesting results in dissociation experiments.[1]

[1] J. R. Hetzler, M. P. Casassa, and D. S. King, J. Phys. Chem. **95**, 8086 (1991).
[2] A. R. W. McKellar, J. K. G. Watson, and B. J. Howard, Mol. Phys. **86**, 273 (1995).
[3] A. Dkhissi, P. Soulard, A. Perrin, and N. Lacome, J. Mol. Spectrosc. **183**, 12 (1997).
[4] J. K. G. Watson and A. R. W. McKellar, Can. J. Phys. **75**, 181 (1997).
[5] F. Legay and N. Legay-Sommaire, Chem. Phys. Lett. **211**, 516 (1993).
[6] R. Kometer, F. Legay, N. Legay-Sommaire, and N. Schwentner, J. Chem. Phys. **100**, 8737 (1994).
[7] J. F. Canty, E. G. Stone, S. B. H. Bach, and D. W. Ball, Chem. Phys. **216**, 81 (1997).
[8] M. D. Brookes, A. R. W. McKellar, and T. Amano, J. Mol. Spectrosc. **185**, 153 (1997).
[9] Y. Naitoh, Y. Fujimura, K. Honma, and O. Kajimoto, J. Phys. Chem. **99**, 13652 (1995).

[10] V. Blanchet and A. Stolow, J. Chem. Phys. **108,** 4371 (1998).
[11] I. S. Nandhakumar, Z. Y. Li, R. E. Palmer, and R. Amos, Surf. Sci. **329**, 184 (1995).
[12] M. Pérez Jigato, V. Termath, P. Gardner, N. C. Handy, D. A. King, S. Rassias, and M. Surman, Mol. Phys. **85**, 619 (1995).
[13] Y. Matsumoto, Y. Ohshima, and M. Takami, J. Chem. Phys. **92**, 937 (1990).
[14] A. Tachibana, M. Yamato, T. Suzuki, and T. Yamabe, J. Mol. Struct.: THEOCHEM **231**, 291 (1991).
[15] J. E. Williams and J. N. Murrell, J. Am. Chem. Soc. **93**, 7149 (1971).
[16] T. Vladimiroff, J. Am. Chem. Soc. **94**, 8250 (1972).
[17] S. Skaarup, P. N. Skancke, and J. E. Boggs, J. Am. Chem. Soc. **98**, 6106 (1976).
[18] M. A. Benzel, C. E. Dykstra, and M. A. Vincent, Chem. Phys. Lett. **78**, 139 (1981).
[19] R. D. Bardo, J. Phys. Chem. **86**, 4658 (1982).
[20] J. P. Ritchie, J. Phys. Chem. **87**, 2466 (1983).
[21] R. D. Harcourt, J. Mol. Struct.: THEOCHEM **206**, 253 (1990).
[22] Y. Mo and Q. Zhang, Int. J. Quantum Chem. **56**, 19 (1995).
[23] K. A. Nguyen, M. S. Gordon, J. A. Montgomery, Jr., and H. H. Michels, J. Phys. Chem. **98**, 10072 (1994).
[24] G. Chaban, M. S. Gordon, and K. A. Nguyen, J. Phys. Chem. A **101**, 4283 (1997).
[25] W. N. Lipscomb, F. E. Wang, W. R. May, and E. L. Lippert, Acta Crystallogr. **14**, 1100 (1961).
[26] C. M. Western, P. R. R. Langridge-Smith, B. J. Howard, and S. E. Novick, Mol. Phys. **44**, 145 (1981).
[27] S. G. Kukolich, J. Mol. Spectrosc. **98**, 80 (1983).
[28] T. J. Lee, A. P. Rendell, and P. R. Taylor, J. Phys. Chem. **94**, 5463 (1990).
[29] R. González-Luque, M. Merchán, and B. O. Roos, Theor. Chim. Acta **88**, 425 (1994).
[30] A. Stirling, I. Pápai, J. Mink, and D. R. Salahub, J. Chem. Phys. **100**, 2910 (1994).
[31] B. S. Jursic and Z. Zdravkovski, Int. J. Quantum Chem. **54**, 161 (1995).
[32] W. A. Guillory and C. E. Hunter, J. Chem. Phys. **50**, 3516 (1969).
[33] T.-K. Ha, Theor. Chim. Acta **58**, 125 (1981).
[34] J. Mason, J. Chem. Soc. (Dalton) **1975**, 19.
[35] F. R. Gilmore, J. Quant. Spectrosc. Radiat. Transf. **5**, 369 (1965).
[36] E. Miescher and K. P. Huber, in *Intern. Rev. Sci., Phys. Chem. Ser. 2, Vol. 3, Spectroscopy*, edited by D. A. Ramsay (Butterworths, London, 1976), pp. 37–73.
[37] K. P. Huber and M. Vervloet, J. Mol. Spectrosc. **129**, 1 (1988).
[38] K. P. Huber and G. Herzberg, *Constants of Diatomic Molecules* (Van Nostrand, New York, 1979).
[39] The 11.0 eV location of the lowest ionic asymptote was obtained from HF-SCF calculation of NO^- and NO^+ with the cc-pVTZ basis set, with the NO bond length of Fig. 3.
[40] MOLPRO94 is a package of *ab initio* programs written by H.-J. Werner and P. J. Knowles with contributions from J. Almlöf, R. D. Amos, M. J. O. Deegan, S. T. Elbert, C. Hampel, W. Meyer, K. A. Peterson, R. M. Pitzer, A. J. Stone, and P. R. Taylor.
[41] H.-J. Werner and P. J. Knowles, J. Chem. Phys. **82**, 5053 (1985).
[42] P. J. Knowles and H.-J. Werner, Chem. Phys. Lett. **115**, 259 (1985).
[43] W. Kohn and L. J. Sham, Phys. Rev. A **140**, 1133 (1965).
[44] R. J. Bartlett, J. Phys. Chem. **93**, 1697 (1989).
[45] C. Hampel, K. Peterson, and H.-J. Werner, Chem. Phys. Lett. **190**, 1 (1992).
[46] H.-J. Werner and P. J. Knowles, J. Chem. Phys. **89**, 5803 (1988).
[47] P. J. Knowles and H.-J. Werner, Chem. Phys. Lett. **145**, 514 (1988).
[48] A. D. Becke, Phys. Rev. A **38**, 3098 (1988).
[49] C. Lee, W. Yang, and R. G. Parr, Phys. Rev. B **37**, 785 (1988).
[50] B. Miehlich, A. Savin, H. Stoll, and H. Preuss, Chem. Phys. Lett. **157**, 200 (1989).
[51] J. D. Watts, J. Gauss, and R. J. Bartlett, J. Chem. Phys. **98**, 8718 (1993).
[52] P. J. Knowles, C. Hampel, and H.-J. Werner, J. Chem. Phys. **99**, 5219 (1993).
[53] T. H. Dunning, Jr., J. Chem. Phys. **90**, 1007 (1989).
[54] R. A. Kendall, T. H. Dunning, Jr., and R. J. Harrison, J. Chem. Phys. **96**, 6796 (1992).
[55] H.-J. Werner and W. Meyer, J. Chem. Phys. **74**, 5794 (1981).
[56] L. L. Lee, *Molecular Thermodynamics of Nonideal Fluids* (Butterworths, Stoneham, London, 1988).
[57] D. A. McQuarrie, *Quantum Chemistry* (University Science Books, Mill Valley, CA, 1983).
[58] B. S. Jursic, Chem. Phys. Lett. **236**, 206 (1995).